

# A novel three-dimensional mixed bridging–ligand complex [Cu<sub>2</sub><sup>II</sup>(tn)<sub>2</sub>][Fe<sup>II</sup>(CN)<sub>6</sub>]·H<sub>2</sub>O with an unexpected 1,3-diaminopropane bridge

Xiao-Ping Shen<sup>a</sup>, Yi-Zhi Li<sup>a</sup>, Ai-Hua Yuan<sup>b</sup>, Zheng Xu<sup>a,\*</sup>

<sup>a</sup>State Key Laboratory of Coordination Chemistry, Nanjing University, Nanjing 210093, People's Republic of China

<sup>b</sup>School of Material Science and Engineering, Jiangsu University of Science and Technology, Zhenjiang 212003, People's Republic of China

Received 17 June 2005; revised 1 July 2005; accepted 1 July 2005

Available online 18 August 2005

## Abstract

Reaction of K<sub>3</sub>[Fe(CN)<sub>6</sub>] with [Cu(tn)<sub>2</sub>](ClO<sub>4</sub>)<sub>2</sub> (tn = 1,3-diaminopropane) leads to a novel mixed cyano and tn bridged three-dimensional (3D) bimetallic assembly [Cu<sub>2</sub><sup>II</sup>(tn)<sub>2</sub>][Fe<sup>II</sup>(CN)<sub>6</sub>]·H<sub>2</sub>O (**1**), in which each [Fe(CN)<sub>6</sub>]<sup>4-</sup> anion connects six copper(II) cations via six CN<sup>-</sup> groups, whereas each copper(II) cation is linked to three [Fe(CN)<sub>6</sub>]<sup>4-</sup> ions and two other copper(II) ions through Cu–NC–Fe and Cu–tn–Cu linkages, respectively. Magnetic studies reveal weak antiferromagnetic interactions between the nearest Cu<sup>II</sup> (*S* = 1/2) ions through the diamagnetic [Fe(CN)<sub>6</sub>]<sup>4-</sup> anion.

© 2005 Elsevier B.V. All rights reserved.

**Keywords:** Hexacyanoferrate(II); Copper complex; Cyano-bridged complex; Crystal structure; Magnetic properties

## 1. Introduction

Design and construction of polymetallic extended compounds [1,2], which is usually accessible by self-assembly under exceedingly mild conditions, is one of the particularly attractive fields because these compounds have many potential applications for technologically useful magnetic, electronic, optical, electrochemical and catalytic materials. It is well known that the cyanide anion, CN<sup>-</sup>, is able to behave as a bridging ligand at both ends, with carbon and nitrogen atoms between two coordination centers. Recently, cyanide-bridged bimetallic assemblies, derived from [M(CN)<sub>6</sub>]<sup>n-</sup> (M = Fe, Cr, Mn, Co) building blocks and co-ordinatively unsaturated transition metal complexes, have attracted continuous interest and become a subject of a large number of studies [3,4]. These assemblies assume oligonuclear, 1D, 2D and 3D structures and exhibit ferro-, ferri-, and meta-magnetic behavior. Furthermore, since copper(II) normally possesses four-, five-, or six-coordination, it is

anticipated that the coupling of the copper amine complexes with hexacyanometalates can give rise to a large variety of assembled complexes with rich structural architectures and tunable physical properties. For instance, two cyano-bridged 2D assemblies of {[Cu(tn)<sub>2</sub>][Fe<sup>II</sup>(CN)<sub>6</sub>]}·KCl·5H<sub>2</sub>O (**2**) [5] and [Cu(tn)<sub>2</sub>]<sub>2</sub>[Fe<sup>III</sup>(CN)<sub>6</sub>]ClO<sub>4</sub>·2H<sub>2</sub>O (**3**) [6] have been obtained by reaction of [Fe(CN)<sub>6</sub>]<sup>3-</sup> with [Cu(tn)]<sup>2+</sup> and [Cu(tn)<sub>2</sub>]<sup>2+</sup> (tn = 1,3-diaminopropane), respectively, in which, as in all other diamine analogues, the diamine ligand (tn) invariably acts as chelating agent. Recently, using the same building blocks as those in synthesis of complex **3**, we obtained a novel 3D mixed bridging–ligand complex [Cu<sub>2</sub><sup>II</sup>(tn)<sub>2</sub>][Fe<sup>II</sup>(CN)<sub>6</sub>]·H<sub>2</sub>O (**1**), in which the tn bridges two Cu(II) ions, giving rise to a very distinct structure. To the best of our knowledge, this is the first mixed cyano- and diamine-bridged complex. Here we report its synthesis, crystal structure and magnetic properties.

## 2. Experimental

### 2.1. Physical measurements

Elemental analyses for C, H and N were performed at a Perkin–Elmer 240C analyzer. Cu and Fe analyses were

\* Corresponding author. Tel.: +86 2583593133; fax: +86 2583314502.  
E-mail address: zhengxu@netra.nju.edu.cn (Z. Xu).

made on a Jarrell-Ash 1100+2000 inductively coupled plasma quantometer. IR spectra were recorded on a Nicolet FT-170SX spectrometer with KBr pellets in the 4000–400  $\text{cm}^{-1}$  region. EPR measurements at room temperature were performed using a Bruker ER 200-D-SRC 10/12 spectrometer. The magnetic measurements were performed on single crystals using a Quantum Design MPMS-XL SQUID magnetometer. Diamagnetic corrections were made using Pascal's constants. Effective magnetic moments were calculated using the equation  $\mu_{\text{eff}} = 2.828(\chi_M \times T)^{1/2}$ , where  $\chi_M$  is the magnetic susceptibility per formula unit.

## 2.2. Preparations

All chemicals were reagent grade and were used without further purification.  $[\text{Cu}(\text{tn})_2](\text{ClO}_4)_2$  was obtained by mixing  $\text{Cu}(\text{ClO}_4)_2 \cdot 6\text{H}_2\text{O}$  and 1,3-diaminopropane in a 1:2 molar ratio in water.



Complex **1** was obtained as black block single crystals by slow diffusion of two 15  $\text{cm}^3$  aqueous solutions of  $\text{K}_3[\text{Fe}(\text{CN})_6]$  (0.15 mmol) and  $[\text{Cu}(\text{tn})_2](\text{ClO}_4)_2$  (0.15 mmol) through a U-shaped tube containing agar gel at room temperature. The resulting crystals were collected, washed with  $\text{H}_2\text{O}$  and dried in air. Anal. found: C, 28.26; H, 4.50; N, 27.48; Cu, 25.28; Fe, 10.94%.  $\text{C}_{12}\text{H}_{22}\text{Cu}_2\text{FeN}_{10}\text{O}$  requires C, 28.52; H, 4.39; N, 27.72; Cu, 25.15; Fe, 11.05%. IR:  $\nu_{\text{max}}/\text{cm}^{-1}$  3588(s), 3382(m), 3249(s), 3169(m), 2950(w), 2936(w), 2884(m), 2085(vs), 2055(vs), 1607(s), 1470(m), 1189(m), 1137(m), 1104(m), 1068(m), 1047(m), 1030(m), 704(m), 668(m), 584(s), 466(m).

## 2.3. Crystallography

Diffraction data were collected at 293 K on a Bruker SMART APEX CCD area detector diffractometer using graphite-monochromated Mo  $\text{K}_\alpha$  radiation ( $\lambda = 0.71073 \text{ \AA}$ ) with the  $\varphi$  and  $\omega$  scan mode. Empirical absorption correction was made with SADABS. The structures were solved by direct methods and refined by full matrix least-squares techniques based on  $F^2$ . All non-hydrogen atoms were refined with anisotropic thermal parameters. The idealized positions of the hydrogen atoms were located by using a riding model. All computations were carried out using the SHELXTL-PC program package.

Crystal data for **1**:  $\text{C}_{12}\text{H}_{22}\text{Cu}_2\text{FeN}_{10}\text{O}$ ,  $M = 505.33$ , monoclinic, space group  $P21/n$ ,  $a = 7.634(2)$ ,  $b = 10.658(2)$ ,  $c = 12.973(3) \text{ \AA}$ ,  $\beta = 90.21(1)^\circ$ ,  $U = 1055.5(4) \text{ \AA}^3$ ,  $Z = 2$ ,  $D_c = 1.590 \text{ g/cm}^3$ ,  $F(000) = 512$ ,  $\mu = 2.696 \text{ mm}^{-1}$  and  $S = 1.08$ . 5468 reflections measured, 2067 unique ( $R_{\text{int}} = 0.009$ ). The final  $R_1 = 0.0607$  and  $wR_2 = 0.1287$  for 1611 observed reflections [ $I > 2\sigma(I)$ ] and 124 parameters.

## 3. Results and discussion

### 3.1. Synthesis and identification

Using the same building blocks of  $[\text{Fe}(\text{CN})_6]^{3-}$  and  $[\text{Cu}(\text{tn})_2]^{2+}$ , two completely different complexes of  $[\text{Cu}_2(\text{tn})_2][\text{Fe}^{\text{II}}(\text{CN})_6] \cdot \text{H}_2\text{O}$  (**1**) and  $[\text{Cu}(\text{tn})_2]_2[\text{Fe}^{\text{III}}(\text{CN})_6]\text{ClO}_4 \cdot 2\text{H}_2\text{O}$  (**3**) have been obtained depending on the reaction condition. In complex **1**, the  $[\text{Fe}(\text{CN})_6]^{3-}$  was reduced to  $[\text{Fe}(\text{CN})_6]^{4-}$  and the molar ratio Cu:tn was transferred from 1:2 to 1:1, which are similar to those in complex  $\{[\text{Cu}(\text{tn})]_2[\text{Fe}^{\text{II}}(\text{CN})_6]\} \cdot \text{KCl} \cdot 5\text{H}_2\text{O}$  (**2**). However, complexes **1** and **2** show completely different tn coordination modes with an unexpected tn bridging in complex **1**. This further demonstrates the structural diversity of bimetallic assemblies constructed from the versatile copper(II) ions and exhibits the influence of reaction condition on the structure. The reason for this reduction of  $[\text{Fe}(\text{CN})_6]^{3-}$  to  $[\text{Fe}(\text{CN})_6]^{4-}$  remains unclear for the moment. Nevertheless, it should be pointed out that an analogous and unclear reduction process has been shown to occur in the formation of other cyano-bridged  $\text{Fe}^{\text{II}}\text{--M}^{\text{II}}$  ( $\text{M} = \text{Cu}, \text{Ni}$  and  $\text{Mn}$ ) systems from  $\text{K}_3[\text{Fe}(\text{CN})_6]$  building block [7–9].

The IR spectrum of complex **1** shows two strong  $\text{C} \equiv \text{N}$  stretching bands at 2085 and 2055  $\text{cm}^{-1}$ . The low frequencies suggests that complex **1** contains  $[\text{Fe}(\text{CN})_6]^{4-}$  rather than  $[\text{Fe}(\text{CN})_6]^{3-}$  (2042  $\text{cm}^{-1}$  for  $\text{K}_4[\text{Fe}(\text{CN})_6]$  and 2119  $\text{cm}^{-1}$  for  $\text{K}_3[\text{Fe}(\text{CN})_6]$  [9]), as revealed by the X-ray crystallography. The blue shift of  $\nu(\text{C} \equiv \text{N})$  compared with that of  $\text{K}_4[\text{Fe}(\text{CN})_6]$  suggests the formation of cyano-bridges. The presence of the tn ligand is confirmed by bands due to NH stretching vibrations at 3249 and 3382  $\text{cm}^{-1}$ . The X-band EPR spectrum of complex **1** at room temperature (Fig. 1) look axial with two main features attributable to  $g_{\parallel} = 2.25$  and  $g_{\perp} = 2.06$ , which is consistent with the distorted trigonal bipyramidal coordination configuration around Cu(II) ions. The spectrum is devoid of any hyperfine structure or half-field signal.

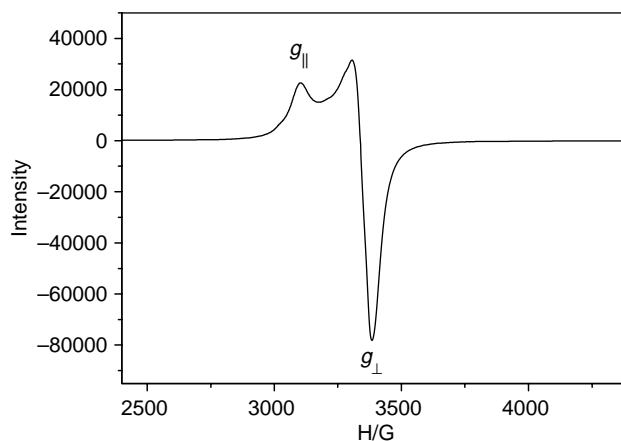


Fig. 1. EPR spectrum of complex **1** at room temperature.

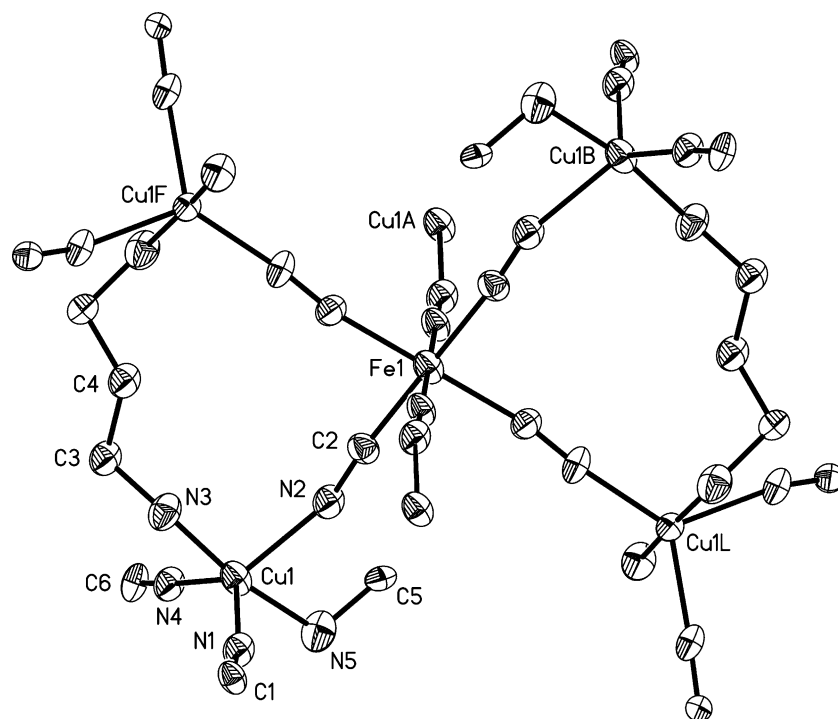


Fig. 2. An ORTEP drawing of complex **1** with the atom numbering scheme. Water molecule is omitted for clarity.

### 3.2. Crystal structure

An ORTEP diagram of complex **1** with the atom numbering scheme is shown in Fig. 2. The unit cell diagram is shown in Fig. 3. The projections along the *a*-axis and *c*-axis are given in Fig. 4. The selected bond distances and angles are listed in Table 1. The molecular structure consists of one  $[\text{Fe}(\text{CN})_6]^{4-}$  anion, one  $[\text{Cu}_2(\text{tn})_2]^{4+}$  unit and one water molecule. An interesting feature of the structure is mixed cyanide and tn bridging mode. Each  $[\text{Fe}(\text{CN})_6]^{4-}$  anion coordinates with six  $\text{Cu}^{2+}$  cations via all six  $\text{C}\equiv\text{N}$  groups, whereas each  $\text{Cu}^{2+}$  cation is linked to three  $[\text{Fe}(\text{CN})_6]^{4-}$  ions and two other  $\text{Cu}^{2+}$  ions through  $\text{Cu}-\text{NC}-\text{Fe}$  and  $\text{Cu}-\text{tn}-\text{Cu}$  linkages, respectively. The  $\text{Cu}^{\text{II}}$  ion assumes a distorted trigonal bipyramid coordination geometry, in which the equatorial sites are occupied by three nitrogen atoms (N1, N2, N4) from  $\text{CN}^-$  groups with the  $\text{Cu}-\text{N}_{\text{eq}}$  bond distances in the range of 1.947(4)–2.080(5) Å, while the axial positions are occupied by two nitrogen atoms (N3, N5) from two tn ligands with  $\text{Cu}-\text{N}_{\text{ax}}$  distances of 1.915(5) and 1.933(5) Å. The  $\text{Cu}-\text{N}_{\text{eq}}$  distances are longer than the  $\text{Cu}-\text{N}_{\text{ax}}$  bond distances, which results in a compressed trigonal bipyramid. The  $\text{Cu}-\text{N}_{\text{eq}}$  bond distances are comparable with the  $\text{Cu}-\text{N}$ (cyanide) distances observed in other cyanometalate analogs [5,8,9]. In addition, the  $\text{Cu}-\text{N}\equiv\text{C}$  bond angles deviate significantly from linearity with the angles of  $\text{Cu1}-\text{N1}-\text{C1}=166.5(4)$ ,  $\text{Cu1}-\text{N2}-\text{C2}=157.6(5)$  and  $\text{Cu1}-\text{N4}-\text{C6}=174.0(5)^\circ$ . The  $[\text{Fe}(\text{CN})_6]^{4-}$  fragment exhibits a distorted octahedral structure. The  $\text{Fe}-\text{C}-\text{N}$  angles and the  $\text{Fe}-\text{C}$  distances range from 169.2(5) to 177.2(5)° and from

1.907(5) to 1.979(5) Å, respectively. In the lattice, Fe and Cu centers linked by cyano-bridges form a rutile-like 3D network with octahedral Fe nodes and trigonal Cu nodes (Fig. 3). The Cu nodes are then crosslinked by the tn bridges to give the overall crystal structure. As shown in Fig. 4a, the 3D network structure in  $\{bc\}$  plane contains a octanuclear  $[-\text{Fe}^{\text{II}}-\text{CN}-\text{Cu}^{\text{II}}-\text{NC}-]_4$  unit, which forms a quadrilateral cavity with four  $\text{Fe}^{\text{II}}$  ions situated at the four corners and four  $\text{Cu}^{\text{II}}$  at the four sides. In the unit, the distances between two adjacent  $\text{Fe}^{\text{II}}$  ions are 9.212(2) and 9.232(3) Å and the distances between two opposite  $\text{Fe}^{\text{II}}$  ions are in the range of 10.658–12.973 Å. The quadrilateral is divided into three parts by two  $\text{Cu}-\text{tn}-\text{Cu}$  bridges, which results in a grid-like

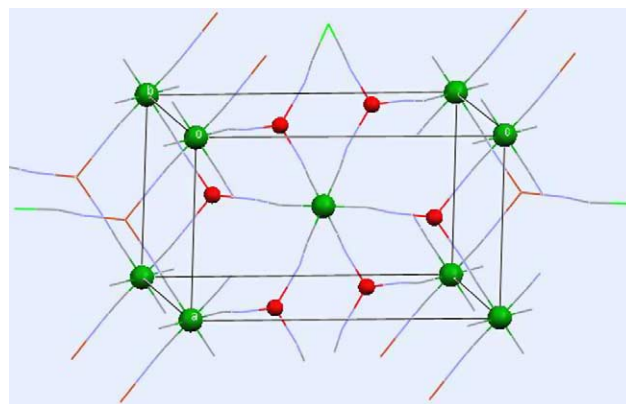


Fig. 3. Unit cell diagram of complex **1** showing rutile-like structure (big ball: Fe; small ball: Cu; Fe and Cu atoms are linked by cyano-bridges).  $\text{H}_2\text{O}$  and tn are omitted for clarity.

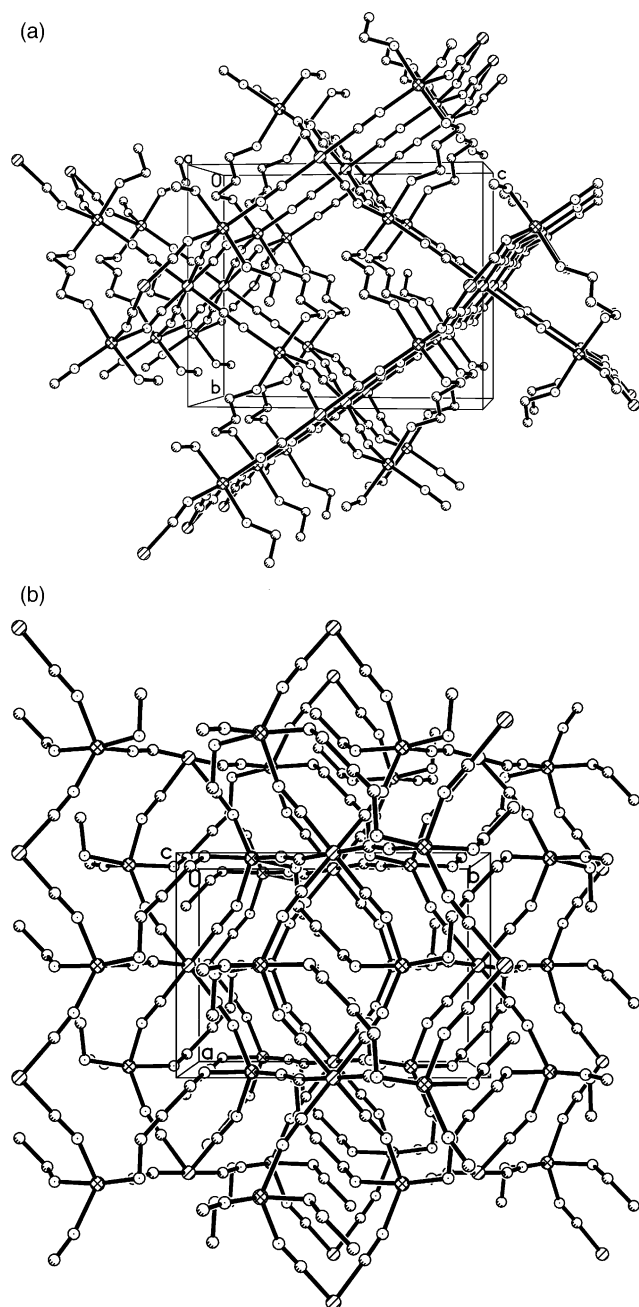


Fig. 4. Projections along the *a*-axis (a) and *c*-axis (b) for complex **1**.

channel structure. From Fig. 4b, a zigzag bilayer can be observed by ignoring the tn bridges. The adjacent bilayers array alternately and are linked by both the cyano-bridges and the tn bridges. So, it can be concluded that the 3D framework of complex **1** is formed by the Fe–C–N–Cu linkages and the structure is further stabilized by the Cu–tn–Cu linkages. The Cu···Fe and Cu···Cu separations along the Fe–CN–Cu linkage range from 5.035 to 5.119 Å and from 10.071 to 10.239 Å, respectively. The adjacent Cu···Cu distance through the tn bridge is 6.784(3) Å. There are weak interactions between the interstitial water molecule (O1) and the cyano nitrogen (N3)[(O1···N3 = 3.176(9) Å] and

Table 1  
Selected bond distances (Å) and bond angles (deg) for complex **1**

Cu1–N1	2.080(5)	Cu1–N2	2.084(5)
Cu1–N3	1.915(5)	Cu1–N4	1.947(4)
Cu1–N5	1.933(5)	Fe1–C2	1.934(6)
Fe1–C1A	1.907(5)	Fe1–C6B	1.979(5)
N1–C1	1.141(7)	N2–C2	1.179(8)
N3–C3	1.420(7)	N4–C6	1.122(7)
N5–C5	1.468(9)	C3–C4	1.437(8)
C4–C5B	1.439(9)		
N1–Cu1–N2	104.8(2)	N1–Cu1–N	388.6(2)
N1–Cu1–N4	129.2(2)	N1–Cu1–N5	95.4(2)
N2–Cu1–N3	93.0(2)	N2–Cu1–N4	125.9(2)
N2–Cu1–N5	78.2(2)	N3–Cu1–N4	92.5(2)
N3–Cu1–N5	171.0(2)	N4–Cu1–N5	91.2(2)
Cu1–N1–C1	166.5(4)	Cu1–N2–C2	157.6(5)
Cu1–N3–C3	136.8(4)	Cu1–N4–C6	174.0(5)
Cu1–N5–C5	112.7(4)	C1A–Fe1–C2	88.4(2)
C2–Fe1–C6B	86.3(2)	C2–Fe1–C2D	180.00
C1E–Fe1–C2	91.6(2)	Fe1E–C1–N1	177.2(5)
C2–Fe1–C6F	93.7(2)	Fe1–C2–N2	174.8(5)
C1A–Fe1–C6B	92.5(2)	C1A–Fe1–C1E	180.00
C6B–Fe1–C6F	180.00	C1A–Fe1–C6F	87.5(2)
Fe1C–C6–N4	169.2(5)		

Symmetry transformations used to generate equivalent atoms:  $A = -1 + x, y, z$ ;  $B = 1/2 - x, -1/2 + y, 3/2 - z$ ;  $C = 1/2 - x, 1/2 + y, 3/2 - z$ ;  $D = -x, 1 - y, 2 - z$ ;  $E = 1 - x, 1 - y, 2 - z$ ;  $F = -1/2 + x, 3/2 - y, 1/2 + z$ .

between the carbon (C5) of the tn ligand and the cyano nitrogen (N2) [C5···N2 = 2.285(9) Å].

### 3.3. Magnetic properties

The magnetic susceptibilities of complex **1** were measured with an applied field  $H = 2$  kOe in the temperature range 2–300 K. The plots of  $\chi_M$  vs.  $T$  and  $\chi_M T$  vs.  $T$  are given in Fig. 5. At room temperature, the  $\chi_M T$  per Cu<sub>2</sub>Fe unit is 0.72 cm<sup>3</sup> K mol<sup>-1</sup> (2.4 μ<sub>B</sub>), which is consistent with the spin-only value of 0.75 cm<sup>3</sup> K mol<sup>-1</sup> (2.45 μ<sub>B</sub>) expected for an uncoupled spin system (two  $S_{Cu} = 1/2$ , one  $S_{Fe} = 0$ ) with  $g = 2.0$ . On lowering the temperature, the  $\chi_M T$  value remains constant down to ca. 20 K, then decreases

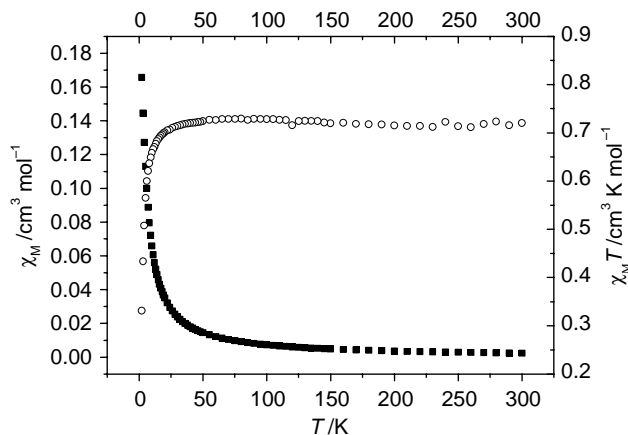


Fig. 5. Temperature dependence of  $\chi_M$  (■) and  $\chi_M T$  (○) for complex **1** measured at 2 kOe.

with further decreasing temperature to  $0.33 \text{ cm}^3 \text{ K mol}^{-1}$  ( $1.63 \mu_{\text{B}}$ ) at 2 K. The magnetic susceptibility above 20 K obeys the Curie–Weiss law with a negative Weiss constant  $\theta = -0.92 \text{ K}$ . These observations suggest the presence of a weak antiferromagnetic interaction in complex **1**, which can be reasonably attributed to the antiferromagnetic coupling between the nearest copper(II) ions through the diamagnetic  $[\text{Fe}(\text{CN})_6]^{4-}$  anions. It has been observed that the  $[\text{Fe}(\text{CN})_6]^{4-}$  ion usually propagates weak ferromagnetic interactions in the  $\text{Ni}^{\text{II}}\text{–Fe}^{\text{II}}$  bimetallic assemblies such as the 3D compound  $[\text{NiL}_2]_3[\text{Fe}(\text{CN})_6](\text{PF}_6)_2$  ( $L = \text{en}, \text{tn}$ ) [10] and the 2D compound  $[\text{Ni}(\text{baepn})]_2[\text{Fe}(\text{CN})_6](\text{H}_2\text{O})_8$  ( $\text{baepn} = N, N'$ -bis(2-aminoethyl)-1,3-propanediamine) [11]. Based on the electronic configurations of  $\text{Ni}(\text{II})$  ( $t_{2g}^6 e_g^2$ ) and  $\text{Fe}(\text{II})$  ( $t_{2g}^6$ ), a  $\sigma$ -superexchange pathway has been proposed between the nearest  $\text{Ni}(\text{II})$  ions through the empty  $d_{\sigma}$  orbital of the  $\text{Fe}(\text{II})$  ion. The  $\text{Ni}(\text{II})\text{–Ni}(\text{II})$  ferromagnetic coupling has been rationalized by taking into account the Goodenough and Kanamori rules [10]. However, for  $\text{Cu}^{\text{II}}\text{–Fe}^{\text{II}}$  bimetallic systems, both ferromagnetic and antiferromagnetic interactions have been reported. For instance, the trinuclear complex  $[\text{Cu}(\text{tren})]_2[\text{Fe}(\text{CN})_6] \cdot 12\text{H}_2\text{O}$  [12], 2D complexes  $[\text{Cu}(\text{dmen})]_2[\text{Fe}(\text{CN})_6]$  ( $\text{dmen} = 2$ -dimethylaminoethylamine) [13] and  $\{[\text{Cu}(\text{tn})]_2[\text{Fe}^{\text{II}}(\text{CN})_6]\} \cdot \text{KCl} \cdot 5\text{H}_2\text{O}$  (**2**) [5] show weak ferromagnetic behavior, while the pentanuclear complex  $[\text{Fe}(\text{CN})_6\{\text{Cu}(\text{dmen})_2\}_4](\text{ClO}_4)_4$  [14] and 1D complex  $[\text{Cu}(\text{L})][\text{Cu}(\text{L}^1)][\text{Fe}(\text{CN})_6] \cdot 6.5\text{H}_2\text{O}$  [ $L = N, N'$ -bis(2-pyridylmethylene)-1,3-propanediamine and  $L^1 = N$ -2-pyridylmethylene-1,3-propanediamine] [9] exhibit weak antiferromagnetic properties. In view of these contradictory results, more examples of  $\text{Fe}^{\text{II}}\text{–Cu}^{\text{II}}$  cyano-bridged complexes are needed in order to clarify the magnetic exchange mechanism. In addition, the FCM (field-cooled magnetization) curve under 10 Oe for complex **1** (Supporting Information, Fig. S1) confirms no magnetic ordering down to 2 K.

#### 4. Conclusion

A novel mixed cyanide and diamine bridged bimetallic assembly,  $[\text{Cu}_2^{\text{II}}(\text{tn})_2][\text{Fe}^{\text{II}}(\text{CN})_6] \cdot \text{H}_2\text{O}$ , has been characterized structurally and magnetically. The complex shows a rutile-like 3D framework structure, which is formed by cyano-bridges and is further stabilized by  $\text{Cu}\text{–tn}\text{–Cu}$  linkages. The peculiar coordination mode of the  $\text{Cu}^{\text{II}}$  ion contributes to the formation of the unexpected interesting structure. The loss of one  $\text{tn}$  ligand from  $[\text{Cu}(\text{tn})_2]^{2+}$  and the remaining  $\text{tn}$  as bridging ligand are entirely unexpected, since the chelating  $\text{tn}$  ligand should form stable  $\text{Cu}^{\text{II}}$  complexes. Both the  $\text{tn}$  bridged compounds [15,16] and the cyano-bridged 3D  $\text{Cu}^{\text{II}}\text{–M}$  ( $M = \text{Fe}, \text{Cr}, \text{Mn}, \text{Co}$ ) assemblies [17,18] are scarcely reported so far. Complex **1** is first example of mixed cyano and diamine-bridged complex and is also a unique example that two

paramagnetic centers are linked through two different types of diamagnetic bridges.

#### 5. Supplementary materials

CCDC 266254 contains the supplementary crystallographic data for this paper. These data can be obtained free of charge via [www.ccdc.cam.ac.uk/conts/retrieving.html](http://www.ccdc.cam.ac.uk/conts/retrieving.html) (or from the Cambridge Crystallographic Data Centre, 12, Union Road, Cambridge CB2 1EZ, UK; fax: +44 1223 336033). FCM (field cooled magnetization vs  $T$ ) curve under 10 Oe and the structure projections along the  $a$ -,  $b$ - and  $c$ -axis are given in Supporting Information.

#### Acknowledgements

This work was supported by the University Natural Science Foundation of Jiangsu Province (04KJB150004) and State Key Laboratory of Coordination Chemistry.

#### Appendix. Supplementary Material

Supplementary data associated with this article can be found, in the online version, at [doi:10.1016/j.molstruc.2005.07.005](https://doi.org/10.1016/j.molstruc.2005.07.005)

#### References

- [1] C.T. Chen, K.S. Suslick, *Coord. Chem. Rev.* 128 (1993) 293.
- [2] O.M. Yaghi, M. O'Keeffe, M. Kanatzidis, *J. Solid State Chem.* 152 (2000) 1.
- [3] M. Ohba, H. Okawa, *Coord. Chem. Rev.* 198 (2000) 313.
- [4] J. Cernak, M. Orendac, I. Potocnak, J. Chomic, A. Orendacova, J. Skorsepa, A. Feher, *Coord. Chem. Rev.* 224 (2002) 51.
- [5] F. Thetiot, S. Triki, J.S. Pala, *New J. Chem.* 26 (2002) 196.
- [6] S.W. Zhang, C.Y. Duan, W.Y. Sun, D.G. Fu, W.X. Tang, *Transition Met. Chem.* 26 (2001) 127.
- [7] R.J. Parker, L. Spiccia, B. Moubaraki, K.S. Murray, D.C.R. Hockless, A.D. Rae, A.C. Willis, *Inorg. Chem.* 41 (2002) 2489.
- [8] R.J. Parker, D.C.R. Hockless, B. Moubaraki, K.S. Murray, L. Spiccia, *Chem. Commun.* (1996) 2789.
- [9] E. Colacio, J.M. Dominguez-Vera, M. Ghazi, R. Kivekas, J.M. Moreno, A. Pajunen, *J. Chem. Soc., Dalton Trans.* (2000) 505.
- [10] N. Fukita, M. Ohba, H. Okawa, K. Matsuda, H. Iwamura, *Inorg. Chem.* 37 (1998) 842.
- [11] J.E. Koo, D.H. Kim, Y.S. Kim, Y. Do, *Inorg. Chem.* 42 (2003) 2983.
- [12] J.H. Zou, Z. Xu, X.Y. Huang, W.L. Zhang, X.P. Shen, Y.P. Yu, *J. Coord. Chem.* 42 (1997) 55.
- [13] N. Mondal, M.K. Saha, B. Bag, S. Mitra, V. Gramlich, J. Ribas, M.S.E. Fallah, *J. Chem. Soc., Dalton Trans.* (2000) 1601.
- [14] C.S. Hong, Y.S. You, *Inorg. Chim. Acta* 357 (2004) 3271.
- [15] I.M. Vezzosi, M. Saladini, *Inorg. Chim. Acta* 100 (1985) 261.
- [16] G. Ciani, M. Moret, A. Sironi, *Inorg. Chim. Acta* 158 (1989) 9.
- [17] H.Z. Kou, S. Gao, J. Zhang, G.H. Wen, G. Su, R.K. Zheng, X.X. Zhang, *J. Am. Chem. Soc.* 123 (2001) 11809.
- [18] X.P. Shen, S. Gao, G. Yin, K.B. Yu, Z. Xu, *New J. Chem.* 28 (2004) 996.